ILLUMINATION INSENSITIVE FACE REPRESENTATION FOR FACE RECOGNITION BASED ON MODIFIED WEBERFACE

Min Yao[1] and Hiroshi Nagahashi[2]
[1]Department of Information Processing, Interdisciplinary Graduate School of Science and Engineering, Tokyo Institute of Technology, Yokohama 226-8503, Japan
[2]Imaging Science and Engineering Laboratory,
Tokyo Institute of Technology, Yokohama 226-8503, Japan

ABSTRACT
Automatic face recognition under varying illumination is a challenging task. Numerous illumination insensitive face representation methods were developed to tackle the illumination problem. Weberface has been recently proposed and its robustness to varying illumination was approved both theoretically and experimentally. In this paper, we present two proposals which improve the conventional Weberface in specific ways and derive an oriented Weberface and largely-scaled Weberfaces. The oriented Weberface takes advantages of the detailed information along various directions within the neighbourhood of a pixel. It concatenates eight directional face images calculated according to the Weber's law. The largely-scaled Weberfaces are created based on the fact that the "local" operation in illumination insensitive feature extraction does not necessarily correspond to the "nearest" neighborhood. It computes the facical features at larger scales than the conventional Weberface. These modifications are aimed at better face representations which are capable of suppressing the illumination influence while maintaining useful facial features. Through the experiments on three databases, we demonstrate large performance improvements (in terms of recognition rates) by the proposed methods, compared with the conventional Weberface. Our methods also yield better results than several state-of-the-art methods.

KEYWORDS: *Face Recognition, Illumination Insensitive, Face Representation, Oriented Weberface, Largely-scaled Weberfaces*

I. INTRODUCTION

In the past few decades, face recognition has achieved high-level developments and has become a very active research topic. However, in real face recognition applications, varying illumination tends to significantly affect the appearance of faces and leads to unsatisfactory performance of a face recognition system [1], [2]. To solve the illumination problem of face recognition, numerous methods were proposed [3]–[7]. Most of the existing methods could be sorted into one of the three categories: traditional image processing techniques, face model learning based methods, and illumination insensitive face representation methods.

Histogram equalization [8] and logarithmic transform [9] are two examples of the first category. But the methods of this kind are not able to tackle large differences in illumination of faces since they only adjust the gray level values of the input image without sophisticatedly considering the characteristics of the objects (i.e. faces).

The second category models the illumination variations using large quantity of illumination samples in advance. In [10], the authors introduced an illumination cone to generalize the illumination relationship between a set of face images in fixed poses but under varying illumination in the space of images. In [11], a spherical harmonic model is proposed to represent a low-dimensional linear subspace stretched by the face images of the same subject under varying illumination and expressions.

This category requires much prior knowledge to learn the illumination model and therefore is not practical for real applications.

Recently, vast efforts have been made to develop a new method of the third category, i.e., an illumination insensitive face representation method. Usually, the methods of this kind are associated to the Lambertian reflectance model. A given illuminated face image $I(x,y)$ can be expressed by the reflectance model as $I(x,y)=R(x,y)L(x,y)$, where R denotes the reflectance related to the intrinsic features of a face and L denotes the luminance cast to the face. Since the component R is only related to the individual facial property, it is considered to be illumination invariant. On the other hand, L is commonly assumed to vary slowly in spatial level. Some illumination insensitive features were created by estimating L in the first place and then getting R based on the reflectance model. For example, Multiscale Retinex (MSR) [12] estimates L by smoothing the original face image and obtains the illumination invariant feature R by using the reflectance model. Self quotient image (SQI) [13] also uses a smoothed version as the estimation of L. The smoothing is realized by weighted Gaussian filters. In [14], W. Cheng et al. proposed a method based on Discrete Cosine Transform (DCT), which deems L to be the first n low frequency components of the transformed image. The component R is eventually attained by a subtraction since the input image is firstly projected into the logarithmic domain. Later, by applying adaptive smoothing, ASR [15] was developed to estimate L more effectively. However, this kind of indirect measure of R will inevitably incur errors during the estimation of L, which is likely to lead these methods to being unrobust to varying illumination. It is argued in [5] that the direct representation of faces only related to R is more effective and robust for illumination insensitive face recognition and a new method called Gradientface (GRF) was proposed in correspondence. It yields better performance than a lot of earlier works. In [16], Weberface (WF) was developed and achieved satisfactory performance as comparable as Gradientface. But the operation employed in Weberface considered only one small scale and ignored the detailed information of face images oriented along different directions which is supposed to be important for face classification.

In this paper, regarding the limitations of the conventional WF, we propose to improve it in two ways to further exploit the capacity for suppressing the illumination influence while maintaining useful facial features. The oriented Weberface (OWF) and largely-scaled Weberfaces are created. The former one calculates eight directional face images separately and then concatenates them to obtain the final output. The latter are produced to get face representations at proper scales. We compare our methods with the conventional Weberface and several other state-of-the-art methods based on three databases. Experimental results show that the proposed methods can achieve fairly encouraging results, outperforming other methods.

In the rest of this paper, we start with a brief introduction about the conventional Weberface in Section II. In Section III, we explain and analyze the proposed methods in detail. In Section IV, the experimental results are presented and discussed. The final conclusion is made in Section V.

II. REVIEW OF WEBERFACE

Weberface [16] is inspired by the Weber's law which supposes that the relative value is more constant than the absolute value. Concretely speaking, it hypothesizes that the ratio between the smallest sensible change in a stimulus ($\Delta I_{\min}$) and the stimulus with noise (I) is a constant:

$$\frac{\Delta I_{\min}}{I} = k . \tag{1}$$

When applied to the illumination insensitive representation of faces, the smallest sensible change is described by the local variation and the noised stimulus corresponds to the illuminated face image. The resultant constant k is the expected illumination insensitive representation. Along this line, Weberface is given by

$$WF = \arctan\left(\alpha \sum_{i=0}^{P-1} \frac{x_c - x_i}{x_c} \right), \tag{2}$$

where x_c denotes the center pixel and x_i (i=0, 1,…, P-1) are its neighboring pixels. Therefore, x_c-x_i describes a local variation. P denotes the total number of the pixels in the neighborhood and α is a

parameter controlling the extent of the local intensity contrast. The arctangent operation is used to avoid the extremely large output. The conventional Weberface sets P as 9, which demonstrates a 3×3 mask for the local operation. The mask is shown in Fig. 1. Also, α=4 proved to be the best according to the experiments in [16].

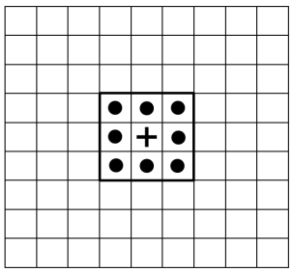

Figure 1. The local operation area using the 3×3 mask.

III. PROPOSED METHODS

In this section, we present the two proposed modifications about the conventional Weberface which generate the oriented Weberface and largely-scaled Weberfaces. These two methods are explained and analyzed in the following consecutive subsections separately.

3.1. Oriented Weberface (OWF)

From (2), one can know that the difference of intensities within a local neighborhood is critical for maintaining the intrinsic facial features and removing the illumination. Facial features and illumination vary in different way along different directions. However, the conventional Weberface summarizes all the results of the subtraction and division within the neighborhood along different directions together. As a consequence, the facial details oriented in variant directions are blurred.

To overcome this drawback of the conventional Weberface, we compute the Weberface along eight different directions. Let O_i (i=1,2,…,8) denote the eight directional face images, then they can be expressed by

$$O_i = \arctan\left(\alpha \frac{x_c - x_i}{x_c} \right)\Bigg|_{i\in\{1,2,3,4,5,6,7,8\}}, \tag{3}$$

where x_c denotes the center pixel, x_i denotes one of the neighboring pixels of x_c. Then these eight directional face images are concatenated to form the final illumination insensitive face representation. We call this representation as an oriented Weberface (OWF) and state it as

$$\begin{aligned} OWF &= \oplus\{O_i\} \\ &= \oplus\left\{ \arctan\left(\alpha \frac{x_c - x_i}{x_c} \right) \right\}\Bigg|_{i\in\{1,2,3,4,5,6,7,8\}}, \end{aligned} \tag{4}$$

where $\oplus\{\cdot\}$ denotes the concatenating operation.

Figure 2 illustrates the proposed OWF. The arrows in this figure show the eight directions and the right-most image gives the eight directional face images O_1 to O_8 of the given image corresponding to the eight directions. Since OWF is based on the Weber's law, it keeps all the merits of Weberface. For example, each of the directional face images is computed as a ratio and thus it is robust to multiplicative noise. On the other hand, the oriented patterns have already had good applications to the face recognition in the literature. For instance, the oriented facial information was also considered in [17] and a new method called oriented local histogram equalization (OLHE) was successfully developed. It was applied to maintain facial features while compensating varying illumination.

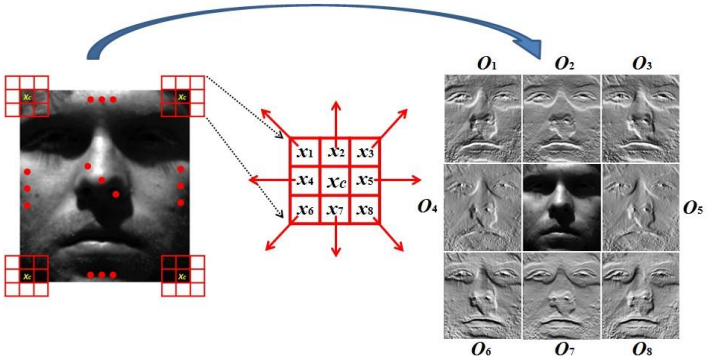

Input face image 3×3 mask Eight directional images

Figure 2. Illustration of OWF.

We have mentioned in the introduction that many illumination invariant facial features are associated to the reflectance model which is expressed as

$$I(x,y) = R(x,y)L(x,y)\,, \tag{5}$$

where $I(x,y)$ denotes the image pixel with illumination, $R(x,y)$ is the reflectance only depending on the intrinsic facial features which is considered to be illumination invariant, and $L(x,y)$ denotes the illumination component at the present pixel (x,y). Next, we would like to prove that OWF is only related to $R(x,y)$ and verify that OWF can represent faces in an illumination insensitive way.
According to (3), each of the directional face images can be rewritten as

$$O_i(x,y) = \arctan\left(\alpha \frac{I(x,y) - I(x+\Delta x, y+\Delta y)}{I(x,y)}\right), \tag{6}$$

where i=1,2,…,8 and $(\Delta x, \Delta y)$ equals to (-1,-1), (-1,0), (-1,1), (0,-1), (0,1), (1,-1), (1,0), and (1,1), respectively when i changes from 1 to 8.
From (5), we have

$$I(x+\Delta x, y+\Delta y) = R(x+\Delta x, y+\Delta y)L(x+\Delta x, y+\Delta y)\,. \tag{7}$$

Since L is commonly assumed to vary very slightly, it is approximately constant within local neighborhood, that is

$$L(x+\Delta x, y+\Delta y) \approx L(x,y)\,. \tag{8}$$

Then the following deduction can be made:

$$\begin{aligned} O_i &\approx \arctan\left(\alpha \frac{R(x,y)L(x,y) - R(x+\Delta x, y+\Delta y)L(x,y)}{R(x,y)L(x,y)}\right) \\ &\approx \arctan\left(\alpha \frac{R(x,y) - R(x+\Delta x, y+\Delta y)}{R(x,y)}\right). \end{aligned} \tag{9}$$

It can be noticed from (9) that each of the directional face images of OWF only depends on the reflectance component R. By concatenating, the final representation of OWF is also only related to R. This indicates that our method is illumination insensitive. Besides the characteristic of being insensitive to illumination changes, OWF contains the detailed facial features along various directions. These features are useful for discriminating between different subjects, which was, made obscure in the conventional Weberface. On the other hand, note that illumination has different influences along different directions. For example, shadow is likely to enforce negative effects along the boundaries. In this case, separate computation of directional face images can disperse the negative effects. Some visual samples of OWF are shown in Fig. 3. It can be seen that our method is able to absorb the specific influence of illumination such as negative effects of shadow boundaries around eyes and nose.

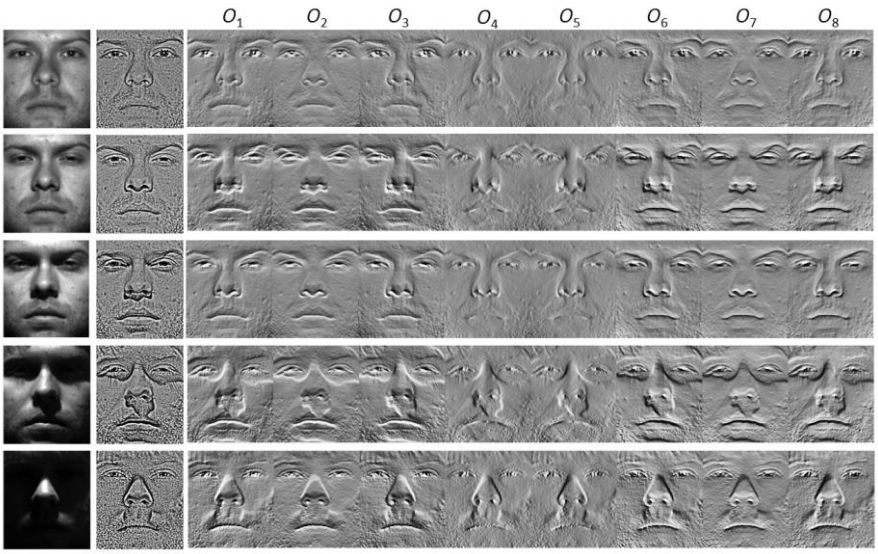

Figure 3. The input face images (1st column), the conventional Weberface (2nd column) of corresponding faces, and the eight directional face images of OWF (3rd column) of corresponding faces.

3.2. Largely-scaled Weberfaces

Theoretically, the illumination component *L* varies slowly in the local area, and this indicates that *L* remains approximately the same within the small neighborhood. Based on this theoretical premise, Weberface was proved to be only related to illumination invariant component *R*. It can be also concluded from this premise that the smaller area the operation is executed in, the more illumination-insensitive the face representation is. Thus, the conventional Weberface uses the operation within a 3×3 squared neighborhood.

However, in real applications, the illumination conditions are far more complex than the simulations given by a physical model. In fact, the "local" operation in illumination insensitive feature extraction does not necessarily correspond to the "nearest" neighborhood. One evidence is found in local normalization (LN) [18]. LN adopted the common assumption about the invariability of *L* in local small area, but finally demonstrated that the best performance was achieved by using the block of size 7 among the sizes of {3, 5, 7, 9, 11, 13}. Moreover, in [19], the analysis of pattern description scales of the proposed methods called Weber local descriptor (WLD) was provided. The developed multiscale WLD improved the discrimination of the original one. Hence, keeping this fact in mind, we are motivated to apply more largely-scaled various masks to gain face representations at proper scales which can realize a good balance between illumination compensation and facial feature maintenance.

In this paper, three largely-scaled Weberfaces are derived using the masks shown in Fig. 4. We name them WF2, WF3, and WF4 corresponding to the mask dimension of 5, 7, and 9, respectively. They are used to characterize the illumination insensitive patterns with local salient facial features in different granularities. In Fig. 4, the pixels represented by the solid black dots are taken as the neighborhood pixels and the center cross represents the pixel under consideration. Actually, simply enlarging the value of *p* in (2) is a way to make scales larger as well. However, this is likely to overlap the smaller scale mask into the larger one and mix the contributions of differently scaled patterns to insensitivity to varying illumination. The computation of these largely-scaled Weberfaces is almost the same with the conventional one. But we find that the increase of the mask size is often accompanied by the larger intensity difference visually. Since the parameter α is used to adjust the intensity difference between neighboring pixels, we slightly decrease the α value for our method with larger mask dimension, that is, α=3 for WF2, α=2 for WF3, α=1 for WF4. Figure 5 gives several visual samples using the conventional Weberface and the largely-scaled Weberfaces, from which we can see that the largely-scaled Weberfaces could reduce most illumination effects and make the important facial features mare salient than the conventional Weberface. According to the analysis of the largely-scaled Weberfaces, they also keep the merits of the conventional one and are only related to the component *R*.

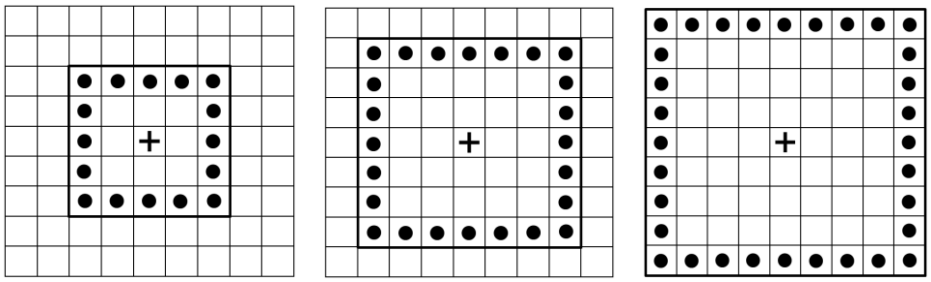

Figure 4. Masks used in the largely-scaled Weberfaces with the dimension of 5, 7, and 9, respectively (from left to right).

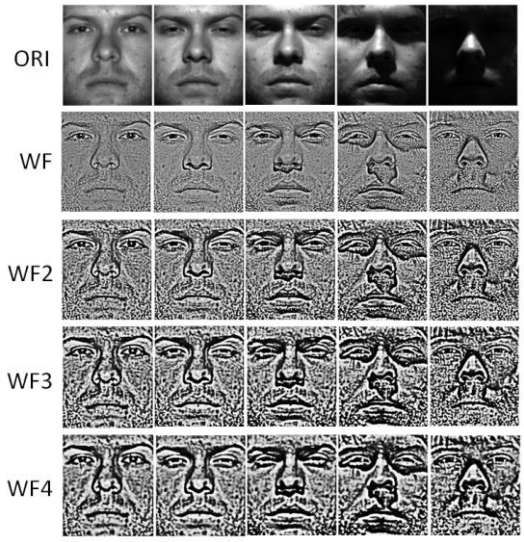

Figure 5. The original face images and their corresponding images processed by the conventional WF, largely-scaled WF2, WF3, WF4 (from top row to bottom row).

IV. EXPERIMENTAL RESULTS AND DISCUSSIONS

In order to evaluate the proposed methods, some experiments were conducted. Assessment is based on three famous databases with large illumination variations, namely CMU-PIE database [20], Yale B Face Database [10] and Extended Yale B Face Database [21]. Several other methods were included for comparison in our experiments.

With regard to the OWF, one can apply PCA for the purpose of dimension reduction. But in our experiments, we used the raw pixel intensities as we did for all the other methods in order to maintain fair comparisons. During the experiments, we used one nearest neighborhood rule with three distance measures—L_1 norm, L_2 norm, and χ^2 distance measure. These measures are defined by the following three equations, respectively.

$$\mathrm{L}_1(\mathbf{X},\mathbf{Y}) = \sum_{i,j} \left| X_{i,j} - Y_{i,j} \right| \tag{10}$$

$$\mathrm{L}_2(\mathbf{X},\mathbf{Y}) = \sqrt{\sum_{i,j} (X_{i,j} - Y_{i,j})^2} \tag{11}$$

$$\chi^2(\mathbf{X},\mathbf{Y}) = \sum_{i,j} \frac{(X_{i,j} - Y_{i,j})^2}{2(X_{i,j} + Y_{i,j})} \tag{12}$$

We selected the best performance result from these three distance measures for each of the tested methods as its result for comparison. The results of the original face images without any processing (ORI) are also given as the baseline.

4.1. Results on Yale B Face Database

Yale B Face Database is composed of 10 subjects with 9 poses and 64 illumination conditions per pose. We used the cropped version of this database [23] and each face image is of size 168×192. We chose only the frontal faces in our experiments and thus there are totally 640 illuminated face images. They were divided into five subsets according to the lighting angles. The five subsets are: subset 1 (0^o~12^o), subset 2 (13^o~25^o), subset 3 (26^o~50^o), subset 4 (51^o~77^o), and subset 5 (above 78^o). According to this subdivision, there are 70, 120, 120, 140, 190 images in subset 1 to 5, respectively.
Based on these subsets, two experiments were devised. The first experiment was conducted to use all the images from subset 1 as the gallery images, and the other images from subset 2 to 5 as the probe images. We compared OWF, WF2, WF3, WF4 with the conventional Weberface (WF) [16] and several other state-of-the-art methods including HE [8], DCT [14], WA [22], SQI [13], ASR [15] and GRF [5]. Figure 6 shows 10 faces under various illumination conditions and the corresponding illumination insensitive face representations using different methods. Table 1 gives the comparative results for different subsets. The distance measure used to get the highest result for each method is also shown correspondingly. As can be seen, the proposed methods achieve extraordinary

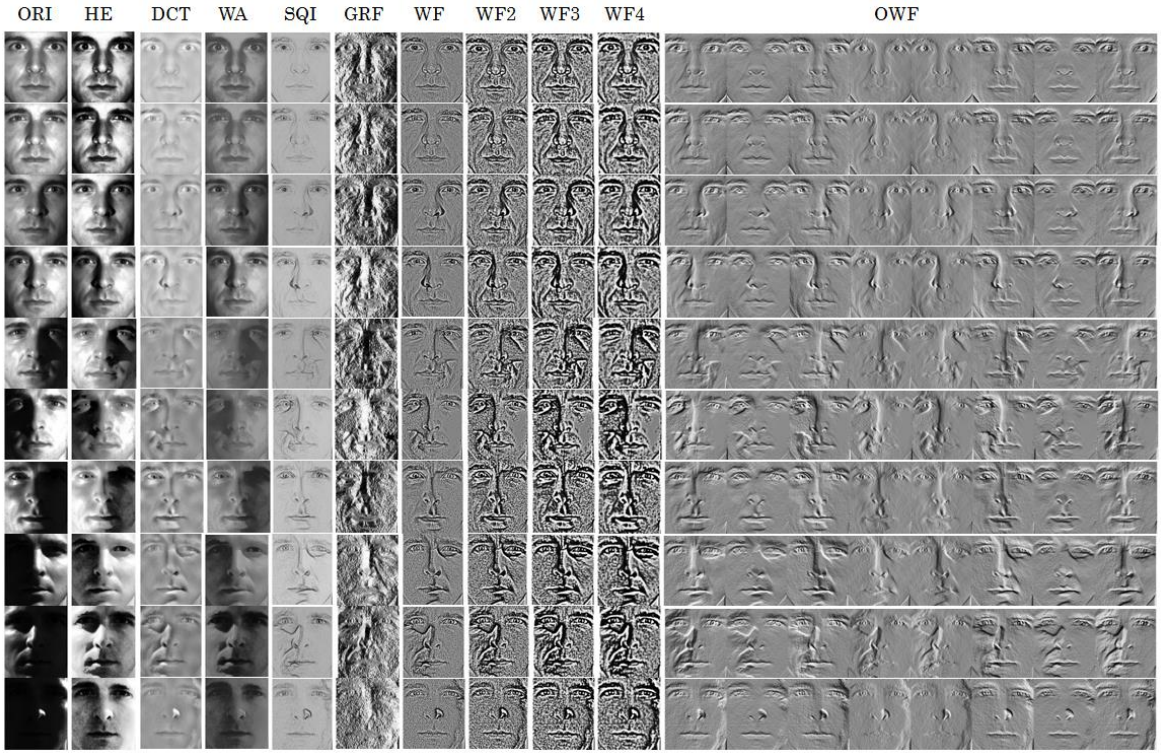

Figure 6. Results of different methods on face images with various illumination in Yale B Face Database. The images are (from left column to right column) face images processed with nothing, HE, DCT, WA, SQI, GRF, WF, WF2, WF3, WF4 and OWF (eight directional face images concatenated together).

performance for face images under harsh illumination conditions of subsets 4 and 5 and the recognition rates for these subsets are all above 99%. As for the average performance, OWF significantly increases the original image with no processing, from 42.81% to 99.83%. WF2, WF3 and WF4 even yield 100.00% recognition rates. They outperform HE, DCT, WA, and SQI greatly. They even get better results than ASR, GRF and the conventional Weberface.

Table 1. Recognition rates (%) on yale B face database with subset 1 as the galleries.

Met.	ORI	HE	DCT	WA	SQI	ASR	GRF	WF	OWF	WF2	WF3	WF4
	χ^2	χ^2	χ^2	χ^2	χ^2	L_1	L_1	L_1	L_1	L_1	$L_1/L_2/\chi^2$	$L_1/L_2/\chi^2$
S2	95.83	100.00	96.67	95.83	90.83	99.17	98.33	97.50	100.00	100.00	100.00	100.00
S3	58.33	90.83	53.33	71.67	87.50	100.00	100.00	100.00	100.00	100.00	100.00	100.00
S4	22.86	41.43	29.29	26.43	88.57	98.57	92.14	98.57	99.29	100.00	100.00	100.00
S5	14.21	63.16	32.11	26.84	90.53	99.47	84.21	100.00	100.00	100.00	100.00	100.00
Avg.	42.81	71.40	49.48	50.70	89.47	99.30	92.45	99.12	99.83	100.00	100.00	100.00

Another experiment based on this database was designed to use one image per subject from subset 1 as the gallery images (totally 10 images). These images are with the most neutral lighting condition. Then the rest images in subset 1 and all images of subsets from 2 to 5 were used as the probes for testing. This experiment is more challenging than the previous one since the reference information is much less. The statistic results are shown in Table 2. The proposed methods generate the best results again. Note that the results of GRF and WF drop largely from those of the first experiment with the decrease of 9.59% and 5.47%, respectively. By contrast, OWF and WF2 are only 1.42%, 0.79% less than the previous results while WF3 and WF4 both keep the 100.00% recognition rates. ASR also obtains satisfactory results, but is still not as comparable as our methods. These encouraging results validate the effectiveness of the proposed methods when applied for illumination insensitive face recognition.

Table 2. Recognition rates (%) on yale B face database with one image per subject in subset 1 as the galleries.

Met.	ORI	HE	DCT	WA	SQI	ASR	GRF	WF	OWF	WF2	WF3	WF4
	χ^2	χ^2	L_2	χ^2	χ^2	L_1	L_1	L_1	L_1	L_1	L_1/χ^2	L_1/χ^2
S1	100.00	100.00	98.33	86.67	61.67	100.00	100.00	90.00	100.00	100.00	100.00	100.00
S2	95.00	98.33	94.17	86.67	65.00	100.00	97.50	97.50	100.00	100.00	100.00	100.00
S3	50.83	72.50	69.17	60.83	45.00	100.00	95.00	93.33	100.00	97.50	100.00	100.00
S4	20.71	47.14	25.71	24.29	52.86	96.43	79.29	94.29	95.00	99.29	100.00	100.00
S5	15.26	54.74	14.21	16.84	48.95	96.32	63.16	92.11	98.42	99.47	100.00	100.00
Avg.	46.51	69.05	50.48	46.83	53.34	98.10	82.86	93.65	98.41	99.21	100.00	100.00

4.2. Results on Extended Yale B Face Database

Extended Yale B Face Database consists of 38 subjects, which is an extended version of Yale B Face Database. Each of these subjects was taken under the same conditions as in Yale B and the image size is 168×192 [23]. We also divided this database into 5 subsets according to the various lighting angles. But the number of images in each subset is greatly increased. There are 266, 456, 456, 532, 722 images in subsets from 1 to 5, respectively. With the enlarged numbers of subjects, we further assessed the proposed methods and generated more persuasive results.

We compared the proposed methods with the conventional Weberface, ASR and GRF based on the same two experiments with those carried out on Yale B Face Database. In the first experiment, subset 1 was used for reference and the other subsets were used for testing. The second experiment used 38 neutrally illuminated images (one image per subject) from subset 1 as the galleries and the rest images in subset 1 together with subsets 2 to 5 for testing. The corresponding comparative results are shown in Tables 3 and 4. In Table 3, it can be seen that the proposed methods get the highest results and the performance of ASR drops largely compared with that on Yale B face database. The second experiment is rather challenging because the number of subjects to be discriminated become more and available reference information is less. However, from Table 4, OWF improves the conventional WF by 14.20% and still maintains the high recognition rate above 90%. The largely-scaled Weberfaces, especially WF3, also significantly outperform the other methods. These results again verify the capability of the proposed methods in illumination insensitive face representation and illustrate their advantages over WF.

Table 3. Recognition rates (%) on extended yale B face database with subset 1 as the galleries.

Met.	ORI	ASR	GRF	WF	OWF	WF2	WF3	WF4
	L_2	L_2	L_1	L_1	L_1	L_1	L_1	L_1
S2	90.13	98.90	99.34	98.03	100.00	99.78	100.00	100.00
S3	41.89	99.56	99.78	99.78	100.00	99.78	99.78	99.78
S4	5.45	91.54	85.90	90.98	98.31	97.74	98.87	99.44
S5	2.63	90.72	59.14	93.21	98.20	96.26	97.92	98.61
Avg.	30.01	94.50	82.73	95.06	98.98	98.11	98.98	99.35

Table 4. Recognition rates (%) on extended yale B face database with one image per subject from subset 1 as the galleries.

Met.	ORI	ASR	GRF	WF	OWF	WF2	WF3	WF4
	χ^2	L_1	L_1	L_1	L_1	L_1	L_1	L_1
S1	95.18	85.09	85.96	65.35	89.47	78.51	82.46	82.89
S2	91.45	99.34	99.34	97.15	100.00	99.56	100.00	91.89
S3	21.49	80.48	84.43	67.98	86.40	77.41	81.58	79.61
S4	4.70	80.64	67.67	76.13	90.79	89.47	93.42	90.60
S5	2.77	73.82	30.06	73.82	89.06	82.69	86.15	90.86
Avg.	32.46	82.54	67.29	76.86	91.06	86.01	89.18	88.10

4.3. Results on CMU-PIE Database

CMU-PIE face database consists of 68 subjects under large variations in illumination, pose and expression, totally 41368 face images. The illumination subset ("C27," 1425 images) of 68 subjects under 21 different illumination directions was chosen in our experiments. All the images were cropped to the size of 161×161. One image per subject (totally 68 images) was chosen as the galleries each time and the others were used as the probes. Figure 7 shows the recognition rates of different methods versus variant gallery images. The results of ORI are excluded from this figure for convenient display purpose due to its rather poor performance. It is noteworthy that the largely-scaled Weberfaces rank the top and can even get good results with harshly illuminated gallery images such as No.1 to 3 and No. 14 to 17. OWF is not as effective but generates better results than ASR, GRF and WF. The average recognition rates of these methods are given in Table 5, which also demonstrates the effectiveness of our methods.

V. CONCLUSIONS AND FUTURE WORK

Face representation for recognizing faces under varying illumination is a task attempting to not only get representation robust to illumination, but also maintain the intrinsic facial features as much as possible. In this paper, considering that the conventional Weberface ignores the facial information oriented along various directions and only adopts a simple scale operation, we proposed to improve it in specific ways. First, we introduced the oriented Weberface (OWF) which makes use of eight directional face images based on the Weber's law and concatenates these images to build an effective face representation insensitive to illumination. It is only related to the reflectance component *R* according to the reflectance model. Most importantly, it can maintain the detailed facial features oriented along various directions while possessing the ability to cushion some negative influence of illumination. On the other hand, we exploited the effectiveness of operations in larger scales. This was inspired by the fact that the "local" operation in illumination insensitive feature extraction does not necessarily correspond to the "nearest" neighbourhood. As a consequence, we presented three largely-scaled Weberfaces which characterize the illumination insensitive patterns with local salient facial features in different granularities. We tested the effectiveness of our methods based on three famous databases. Our methods improved the original face images by recognition rates above 50%. They also outperformed the conventional Weberface and several state-of-the-art methods significantly. These encouraging results achieved by our methods confirmed their robustness to illumination changes and

justified their contributions to illumination insensitive face recognition. However, the computational cost and memory cost of OWF are rather high and how to combine each of the advantages of our methods remains unsolved. Solving these problems should be the future direction of our research.

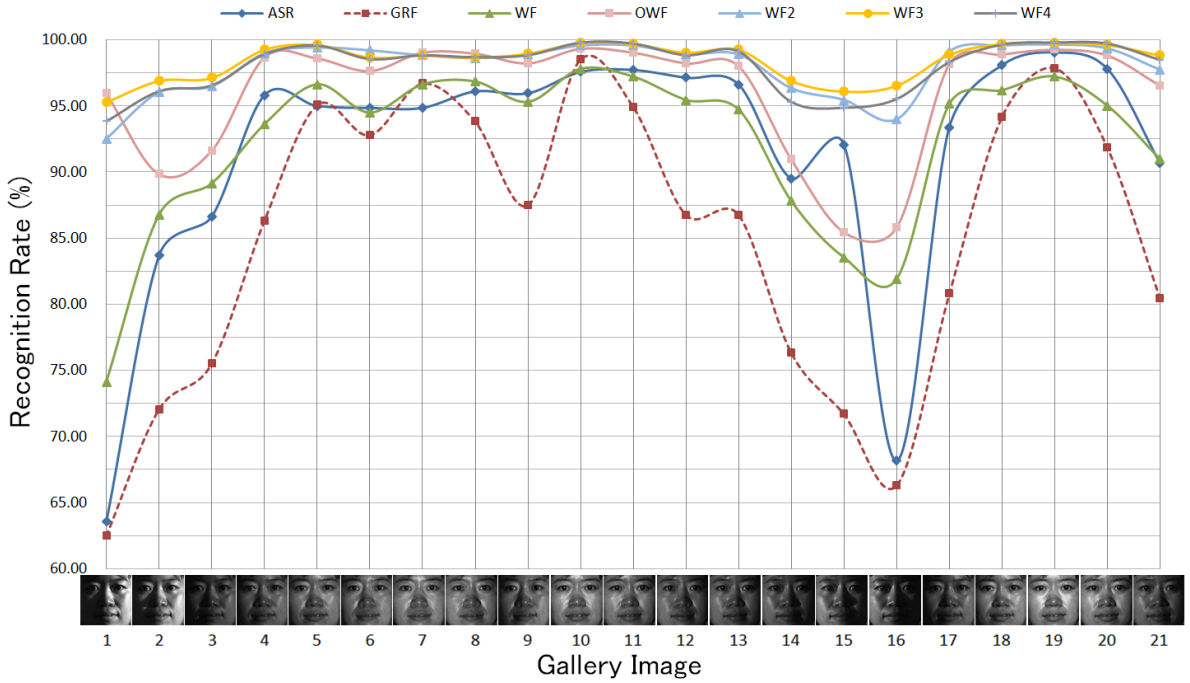

Figure 7. Recognition rates of variant methods on CMU-PIE database using different gallery images (face images of 21 illumination conditions) shown in the horizontal axis.

Table 5. Average recognition rates (%) on CMU-PIE face database.

Met.	ORI	ASR	GRF	WF	OWF	WF2	WF3	WF4
	L_2	L_2	L_1	L_1	L_1	L_1	L_1	L_1
Avg.	28.47	91.62	85.18	92.21	96.05	97.95	98.46	98.04

ACKNOWLEDGEMENTS

Min Yao would like to thank the Ministry of Education, Culture, Sports, Science & Technology in Japan (MEXT) for the financial support during her study in Japan. The authors would like to thank anyone who ever gave instructions, suggestions and supports to this work.

REFERENCES

[1]. P. Phillips, H. Moon, S. Rizvi, and P. Rauss, (2000) "The FERET evaluation methodology for face-recognition algorithms," IEEE Transactions on PAMI, vol. 22, pp. 1090-1104, 2000.
[2]. D. Blackburn, M. Bone, and P. Philips, (2000) "Facial recognition vendor test 2000: evaluation report", 2000.
[3]. X. Zou, J. Kittler, and K. Messer, (2007) "Illumination invariant face recognition: A Survey," IEEE International Conference on Biometrics: Theory, Applications, and Systems, pp. 1–8, 2007.
[4]. V. Struc, J. Zibert, N. Pavesic, (2009) "Histogram remapping as a preprocessing step for robust face recognition," WSEAS Transactions on Information Science and Applications, vol. 3, no. 6, pp. 520–529, 2009.
[5]. T. Zhang, Y. Y. Tang, B. Fang, Z. Shang, and X. Liu, (2009) "Face recongition under varying illumination using Gradientfaces," IEEE Transactions on Image Processing, vol. 18, no. 11, pp. 2599–2606, 2009.
[6]. M. Leszczynski, (2010) "Image preprocessing for illumination invariant face verification," Journal of Telecommunication and Information Technology, vol. 4, pp. 19–25, 2010.

[7]. M. Yao and H. Nagahashi, (2013) "Oriented Weberface for illumination insensitive face representation in face reocngition," IEEE International Conference on Computer Science and Automation Engeering, 2013.
[8]. S. M. Pizer and E. P. Amburn, (1987) "Adaptive histogram equalization and its variations," Computer Vision, Graphics, and Image Processing, vol. 39, no. 3, pp. 355–368, 1987.
[9]. M. Savvides and V. Kumar, (2003) "Illumination normalization using logarithm transforms for face authentication," in Proc. IAPR AVBPA, pp. 549–556, 2003.
[10]. A. S. Georghiades, P. N. Belhumeur, and D. J. Kriegman, (2001) "From few to many: Illumination cone models for face recognition under variable lighting and pose," IEEE Transactions on PAMI, vol. 23, no. 6, pp. 643–660, Jun. 2001.
[11]. R. Basri and D. W. Jacobs, (2003) "Lambertian reflectance and linear subspaces," IEEE Transactions on PAMI, vol. 25, no. 2, pp. 218–233, 2003.
[12]. D. J. Jobson, Z. Rahman, and A. Glenn, (1997) "A multiscale retinex for bridging the gap between color images and the human observation of scenes," IEEE Transactions on Image Processing, vol. 6 (7), pp. 965–976, 1997.
[13]. H. Wang, S. Z. Li, and Y. Wang, (2004) "Face recognition under varing lighting conditions using self quotient image," Proc. IEEE International Conference on Automatic Face and Gesture Recognition, pp. 819–824, 2004.
[14]. W. Cheng, M. J. Er, and S. Wu, (2006) "illumination compensation and normalization for robust face recognition using discrete cosine transform in logarithm domain," IEEE Transactions on System, Man, and Cybernetics, Part B: Cybernetics, vol. 36 (2), pp. 458–466, 2006.
[15]. Y. K. Park, S. L. Park, and J. K. Kim, (2008) "Retinex method based on adapative smoothing for illumination invariant face recognition," Signal Processing, vol. 88, no. 8, pp. 1929-1945, 2008.
[16]. B. Wang, W. Li, W. Yang, and Q. Liao, (2011) "Illumination normalization based on Weber's law with application to face recognition," IEEE Signal Processing Letters, vol. 18, no. 8, pp. 462-465, 2011.
[17]. P. H. Lee, S. W. Wu, and Y. P. Hung, (2012) "Illumination compensation using oriented local histogram equalization and its application to face recognition," IEEE Transactions on Image Processing, vol. 21 (9), pp. 4280–4289, 2012.
[18]. Xudong Xie and Kin-Man Lam, (2006) "An efficient illumination normalization method for face recognition," Pattern Recognition Letters, vol. 27, no. 6, pp. 609-617, 2006.
[19]. J. Chen, Jie, S. Shan, C. He, G. Zhao, M. Pietikainen, X. Chen, and W. Gao, (2010) "WLD: A robust local image descriptor," IEEE Transactions on PAMI, vol. 32, no. 9, pp. 1705-1720, 2010.
[20]. Sim, Terence, Simon Baker, and Maan Bsat, (2003) "The CMU pose, illumination, and expression database." IEEE Transactions on PAMI, vol. 25, no. 12, pp. 1615-1618, 2003.
[21]. K. C. Lee and J. Ho, and D. Kriegman, (2005) "Acquiring Linear Subspaces for Face Recognition under Variable Lighting," IEEE Transactions on PAMI, vol. 27 (5), pp. 684–698, 2005.
[22]. D. Shan and R. Ward, (2005) "Wavelet-based illumination normalization for face recognition," in Proc. IEEE International Conference on Information Processing, vol. 2, 2005.
[23]. http://vision.ucsd.edu/~leekc/ExtYaleDatabase/ExtYaleB.html.

AUTHORS

Min Yao received B.E. from Department of Information Science and Technology, Southeast University, China in 2009 and M.E. from Department of Information Processing, Tokyo Institute of Technology, Japan in 2011, respectively. At present, she is a Ph.D. candidate in Department of Information Processing, Tokyo Institute of Technology. She is being funded by the scholarship of the Ministry of Education, Culture, Sports, Science & Technology in Japan (MEXT). Her research interests include pattern recognition, image processing, and face detection & recognition in difficult conditions.

Hiroshi Nagahashi received his B.S. and Dr.Eng. degrees from Tokyo Institute of Technology in 1975 and 1980, respectively. Since 1990, he has been with Imaging Science and Engineering Laboratory, Tokyo Institute of Technology, where he is currently a professor. His research interests include pattern recognition, computer graphics, image processing, and computer vision.